Pulse Shape Analysis of Enriched BEGe Detectors in Vacuum Cryostat and Liquid Argon

Victoria Wagner

for the GERDA Collaboration

Max-Planck-Institut für Kernphysik

DPG Frühjahrstagung, Dresden, 4.-8. März 2013

BEGe Detectors

Sensitivity to the lower limit of the half life scale of the neutrinoless double beta decay ($0\nu\beta\beta$)

$$T_{1/2} \propto \epsilon a \sqrt{\frac{Mt}{BI\Delta(E)}}$$

ϵ: detection efficiency,
a: abundance of ^{76}Ge
M: mass [kg],
t: exposure time [yr],
BI: background index [$\frac{counts}{keV \cdot kg \cdot yr}$],
$\Delta(E)$: energy resolution in ROI at $Q_{\beta\beta} = 2039$ keV

Broad Energy Germanium (BEGe) detectors as the GERDA Phase II detectors will improve the sensitivity by

- improved energy resolution $\Delta(E)$
- enhanced pulse shape discrimination against background events

This talk focuses on the first seven enriched BEGe detectors

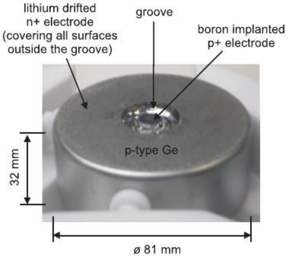

picture from JINST 5 P10007

Which pulse shapes can we distinguish?

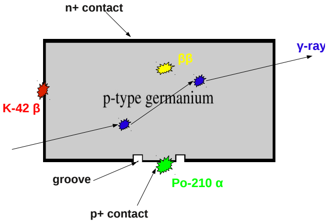

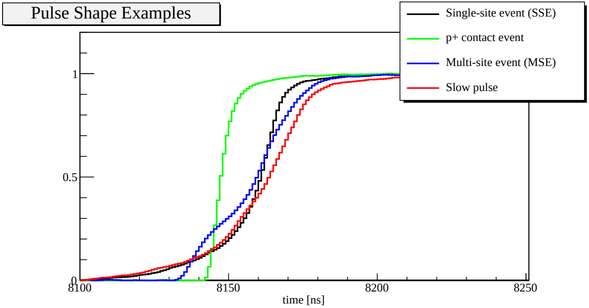

Pulse shape topologies

- $0\nu\beta\beta$-events are single site events (SSE)
- SSE by γ-rays are signal like and cannot be rejected
- γ- rays can interact via multiple Compton scattering (MSE)
- β-particles enter the detector via the n^+ surface and produce slow pulses
- α-particles enter the detector through the region of the p^+ contact producing a comparatively high signal

The Pulse Shape Analysis Method

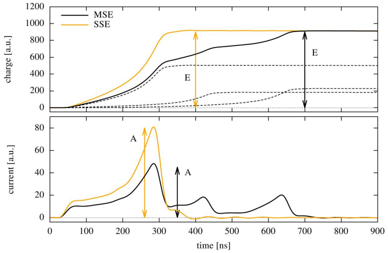

picture from JINST 6 P03005

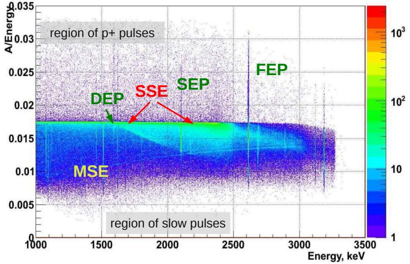

Pulse Shape Analysis (PSA)

- Use the ratio of the amplitude of the current signal A and the energy E: **A/E**
- A/E cut determined in PSA of a ^{228}Th spectrum:
  - SSE are located on a horizontal line
  - MSE are found below the SSE-line
  - single escape peak (SEP) of the 2614.5 keV line contains a high fraction of MSE
  - prominent double escape peak (DEP at 1592.5 keV) of the ^{208}Tl-line at 2614.5 keV, which contains a high fraction of SSE
- Acceptance in DEP is set to 90%

PSA in Vacuum Cryostat

- *A/E* cut determined using the *A/E* distribution in the DEP
- *A/E* distributions of the new enriched BEGe detectors in comparison to a prototype BEGe which is isotopically depleted in ^{76}Ge (in red)

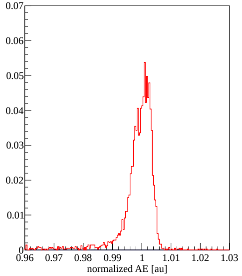

Observations:

expected Gaussian
distribution in the DEP

PSA in Vacuum Cryostat

- A/E cut determined using the A/E distribution in the DEP
- A/E distributions of the new enriched BEGe detectors in comparison to a prototype BEGe which is isotopically depleted in ^{76}Ge (in red)

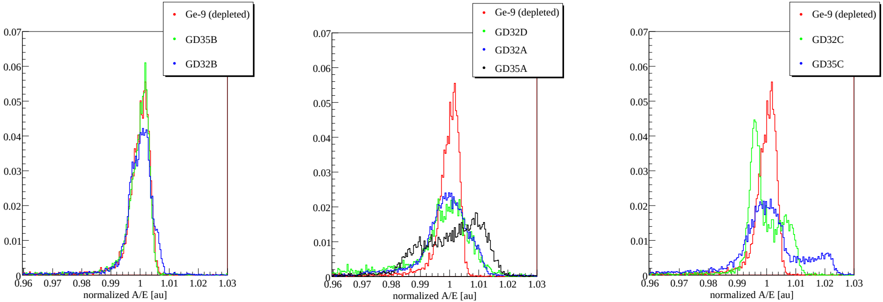

Observations:

2 BEGe detectors show an A/E distribution as expected

3 BEGe detectors show a broadened A/E distribution

2 BEGe detectors show a multi-structure in the A/E distribution

Pulse Shape Discrimination Efficiencies

PSD efficiencies with acceptance in DEP set to 90%

Detector	GD35A	GD32C	GD32A	GD32D
SEP	**0.078 $\pm$ 0.013**	**0.080 $\pm$ 0.017**	**0.121 $\pm$ 0.006**	**0.142 $\pm$ 0.032**
FEP 2.6MeV	0.132 $\pm$ 0.012	0.117 $\pm$ 0.013	0.163 $\pm$ 0.001	0.217 $\pm$ 0.035
1989-2089keV	**0.395 $\pm$ 0.020**	**0.404 $\pm$ 0.029**	**0.427 $\pm$ 0.003**	**0.466 $\pm$ 0.033**

Detector	GD35C	GD35B	GD32B	prototype
SEP	**0.106 $\pm$ 0.023**	**0.056 $\pm$ 0.010**	**0.051 $\pm$ 0.011**	**0.057 $\pm$ 0.016**
FEP 2.6MeV	0.157 $\pm$ 0.020	0.065 $\pm$ 0.010	0.082 $\pm$ 0.011	0.074 $\pm$ 0.014
1989-2089keV	**0.405 $\pm$ 0.028**	**0.322 $\pm$ 0.024**	**0.323 $\pm$ 0.021**	**0.324 $\pm$ 0.035**

Observations:

- Deterioration of PSD efficiency compared to prototype BEGe's (in blue)

Investigation of Pulse Shape Performance

The unexpected A/E distributions cannot be explained by instabilities in time or contributions arising from measurement setup, i.e. electronics and DAQ system, or high level of noise

Investigation of Pulse Shape Performance

The unexpected A/E distributions cannot be explained by instabilities in time or contributions arising from measurement setup, i.e. electronics and DAQ system, or high level of noise

Working hypothesis: Distortion of the electric field inside the diodes

- The charge carriers follow the electrical field: Holes are collected in the middle plane of the detector and funneled towards the read-out electrode – *"Funneling Effect"*
- The funneling ensures that all drift paths of charge carriers are similar, resulting in similar pulse shapes – thus A/E – regardless of different interaction points
- Changes in the internal electrical field might destroy the *"Funneling Effect"* and lead to position-dependent A/E values
- The internal electrical field might be distorted by surface effects, such as charges in the detector groove

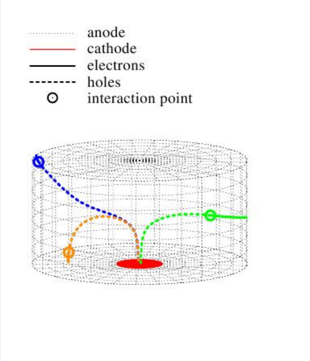

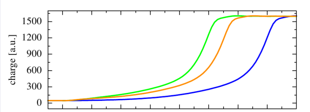

pictures taken from JINST 6 P03005

Investigation of the A/E Position-Dependence

- Different measurements were performed with a collimated ^{241}Am source at different azimuthal angles and the center position
- For the 59.5 keV γ-line the Photoeffect is dominant i.e. mainly SSE

Deviation in A/E peak position compared to the center position [%]

azimuthal	GD32C	GD35A	**GD32B**	**prototype**
0 deg	2.88	-0.03	**0.35**	**0.04**
90 deg	2.25	0.85	**0.82**	**0.08**
180 deg	1.85	2.36	-	**0.04**
270 deg	2.78	0.46	**0.19**	**0.08**

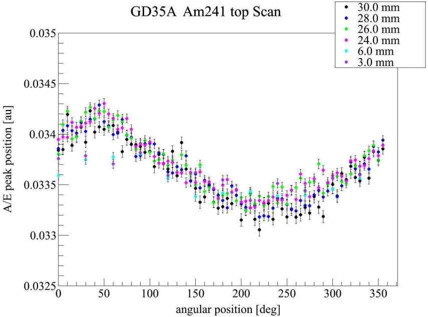

Observations:

- Detectors with good pulse shape performance show a position dependence in A/E smaller than 1% (in bold)
- Detectors with deteriorated PSD efficiency show a large position dependence in A/E
- No correlation found between the structure of the A/E distribution in the DEP and the A/E position-dependence

Reprocessing of Diodes

- If the deterioration in pulse shape performance is related to surface effects a mechanical and chemical treatment of the detectors surface should change the A/E distribution
- For two detectors the passivation layer in the detector groove was renewed

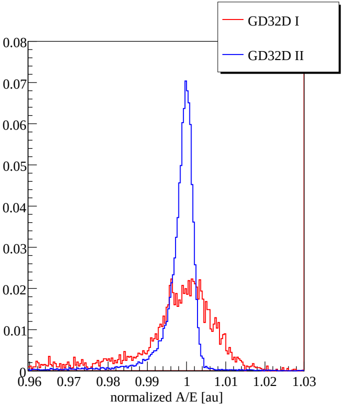

PSD Efficiencies before and after surface treatment

Detector	GD32D I	GD32D II
SEP	**0.142 $\pm$ 0.032**	**0.059 $\pm$ 0.004**
FEP 2.6 MeV	0.217 $\pm$ 0.035	0.077 $\pm$ 0.001
1989-2089 keV	**0.466 $\pm$ 0.033**	**0.377 $\pm$ 0.003**

Observations:

- Resolution of A/E distribution in DEP improved from 1.6% before (I) to 0.5% after (II) the reprocessing
- Improvement in PSD efficiency achieved by the surface treatment
- Strong hint that surface effects influence PSA

Pulse Shape Performance in liquid argon (LAr)

- In their final configuration the BEGe detectors will be install in the GERDA LAr cryostat
- The passivation layer in the detector groove will be removed
- Two of the enriched BEGe diodes were tested in LAr without passivation layer (PL)

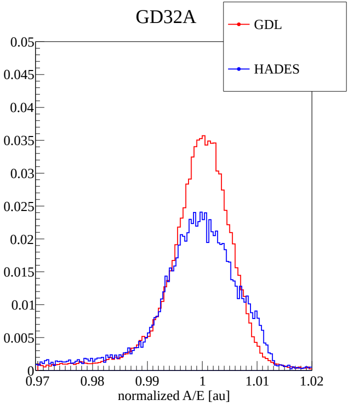

PSD efficiencies	w/o PL	with PL
SEP	**0.082 ± 0.015**	**0.121 ± 0.006**
FEP 2.6MeV	0.115 ± 0.011	0.163 ± 0.001
1989-2089 keV	**0.380 ± 0.030**	**0.427 ± 0.003**

Observations:

- Both diodes show an improvement in A/E resolution
- A natural BEGe with PL measured in the same setup shows a comparatively poor A/E resolution

Performance in the GERDA LAr Cryostat

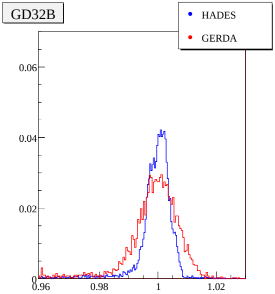

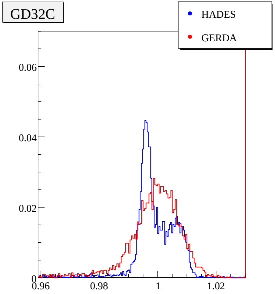

- Five enriched BEGe detectors were installed into the GERDA LAr cryostat prior to the update of Phase II

Pulse Shape Discrimination Efficiencies in GERDA LAr cryostat

Detector	GD32B	GD32C
SEP of 2.6 MeV	**0.110 $\pm$ 0.043**	**0.106 $\pm$ 0.038**
FEP 2.6 MeV	0.136 $\pm$ 0.057	0.131 $\pm$ 0.032
1989-2089 keV	**0.435 $\pm$ 0.067**	**0.441 $\pm$ 0.046**

Observations:

- Multi-structure in A/E distribution vanished
- Broadening of the A/E in the DEP observed for all five BEGe's
- Broadening of the energy resolution due to a higher level of noise compared to HADES setup

PSA in the GERDA LAr Cryostat

- For GERDA the discrimination between SSE and MSE is important as well as the rejection of α- and β- particles
- α's enter the detector at the p$^+$-contact: high A/E value
- β's enter the detector at the n$^+$-contact: low A/E value

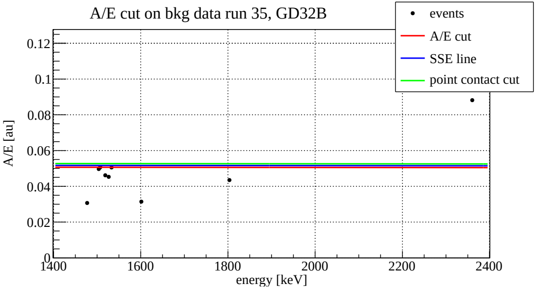

Observations:

- Enriched BEGe detectors show a good performance in GERDA LAr cryostat
- With PSA it is possible to reject efficiently multi-site as well as surface α- and β-particles

Conclusions

- The enriched BEGe detectors show an overall satisfactory pulse shape discrimination.
- The pulse shape discrimination efficiency is influenced by surface effects.
- In vacuum cryostat some enriched BEGe detectors show an unexpectedly high position-dependence of the A/E parameter.
- Standard performance is restored by operation in liquid argon and removal of the passivation layer in the groove.
- With the enhanced pulse shape discrimination properties of the new enriched BEGe detectors it is possible to efficiently suppress background events such as multi-site γ-events as well as surface α- and β-particles.

- The results are promising that the Phase II design background index of $10^{-3} \frac{counts}{keV \cdot kg \cdot yr}$ will be reached with the new enriched BEGe detectors and the LAr veto
- More about the PSD cut in HK66.6

Bonus Slides

More about the background in GERDA

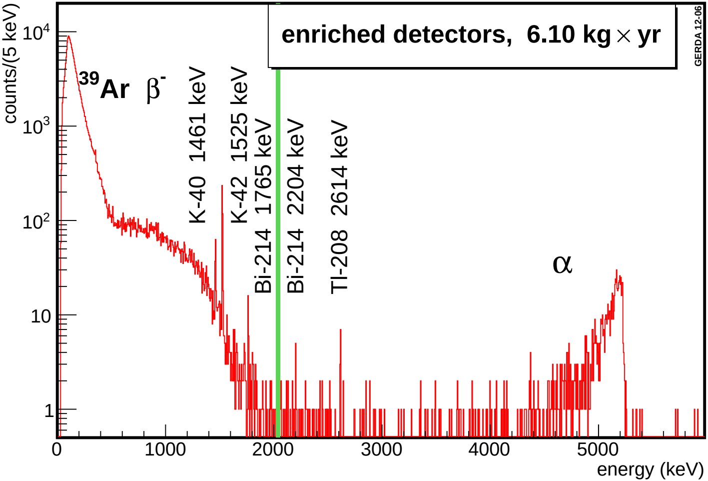

More about the electrical field inside diodes

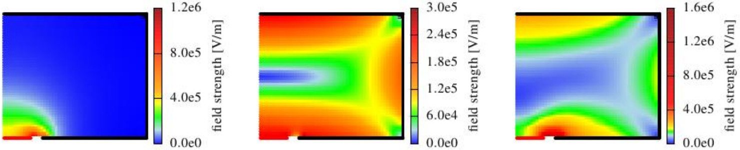

(b) $||\vec{E}_0(\vec{r})||$ (d) $||\vec{E}_\rho(\vec{r})||$ (f) $||\vec{E}(\vec{r})||$

The Funneling Effect from JINST 6 P03005,

The internal electrical field $\vec{E}$ can be understood as a superposition of the potential created by the space charge distributions in the active volume, $\vec{E}_\rho$, and the electric field generated by the electrode potential only, $\vec{E}_0$:

$$\vec{E}(\vec{r}) = \vec{E}_0(\vec{r}) + \vec{E}_\rho(\vec{r})$$

- The electric field created by the electrodes only, $\vec{E}_0$, is weak in the detector but in the vicinity of the small read-out electrode
- whereas $\vec{E}_\rho$ is strongest at the surface and weak in the middle slice of the diode

As the charge clusters follow the electrical field, the holes are collected in the middle slice of the detector, mainly by the contribution from $\vec{E}_\rho$, and finally funneled towards the read-out electrode by $\vec{E}_0$.

More about the signal developing in the diodes

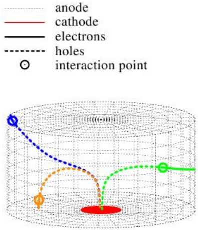

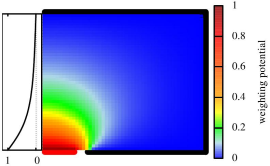

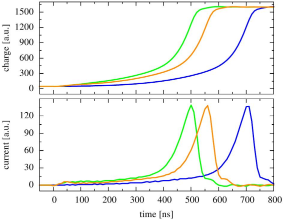

Signal Development from JINST 6 P03005

The charge Q induced by a charge carrier q in the active detector volume at the read-out electrode is described by the Shockley-Ramo theorem:

$Q = -q \cdot W(x)$

$W(x)$ is the so-called *weighting potential* for the charge q at the position x. The signal development in time, i.e. the pulse shape, is given by the weighting potential $W(x)$. The signal increases as the charge cluster reaches a position of strong weighting potential within the diode.

More about the energy and A/E resolution

Detector	Energy resolution in DEP [keV]	Energy resolution in FEP 2.6 MeV [keV]	A/E Resolution in DEP
GD35A	1.87 ± 0.03	2.39 ± 0.01	2.20%
GD32C	1.86 ± 0.04	2.44 ± 0.01	1.27%
GD32A	1.88 ± 0.02	2.44 ± 0.01	1.46%
GD32D	1.86 ± 0.04	2.41 ± 0.02	1.64%
GD35C	1.81 ± 0.03	2.41 ± 0.01	1.70%
GD35B	$\mathbf{1.84 \pm 0.03}$	$\mathbf{2.45 \pm 0.01}$	**0.61%**
GD32B	$\mathbf{1.90 \pm 0.03}$	$\mathbf{2.41 \pm 0.01}$	**0.80%**
prototype	$\mathbf{1.85 \pm 0.03}$	$\mathbf{2.41 \pm 0.01}$	**0.48%**

Energy resolution in DEP and FEP 2.6 MeV for the enriched diodes and depleted Ge-9 as obtained by GELTATIOUtilities. In addition relative resolution of A/E distribution in DEP is shown. For A/E resolution FWHM and mean of a Gaussian fit is used. Uncertainties from fits are negligible. A/E distribution are not pure Gaussian, such that the given resolution is only an estimation.

More about the collimated ^{241}Am Measurements

	GD35A	GD32C	GD32A	GD32D
azimuthal	deviation [%]	deviation [%]	deviation [%]	deviation [%]
0 deg	-0.03	0.53	2.69	-
90 deg	0.82	1.89	2.34	3.29
180 deg	2.36	-	2.35	4.31
270 deg	0.46	0.52	2.80	4.13
	GD35C	**GD32B**	**GD32B**	**depleted**
azimuthal	deviation [%]	deviation [%]	deviation [%]	deviation [%]
0 deg	2.88	**0.35**	**0.35**	**0.04**
90 deg	2.25	**0.65**	**0.82**	**0.08**
180 deg	1.85	-	-	**0.04**
270 deg	2.78	**0.34**	**0.19**	**0.08**

Deviation of A/E peak position from center position for the 7 enriched and the depleted Ge-9 BEGe. A/E peak position for each measurement was extracted from a Gaussian fit of the A/E distribution in the 59.5 keV-line. Measurements were performed with collimated ^{241}Am source at the indicated position on the endcap

More about the detailed ^{241}Am Measurements

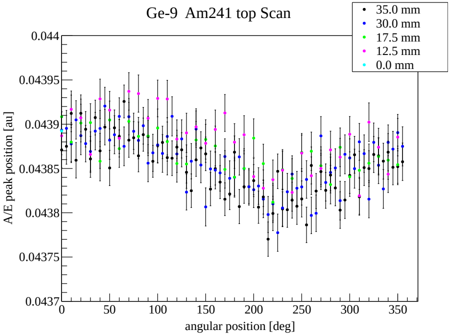

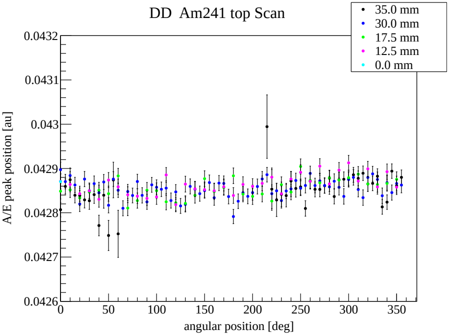

More about the detailed ^{241}Am Measurements

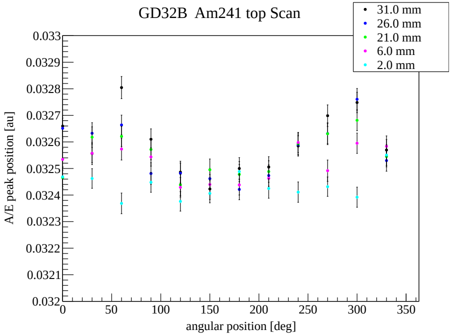

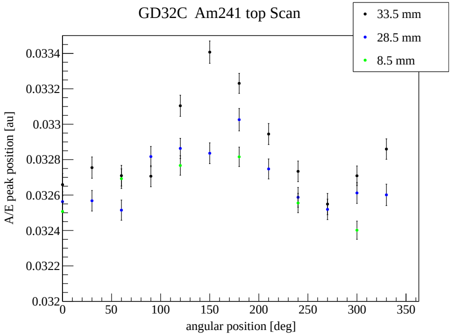

More about the detailed ^{241}Am Measurements

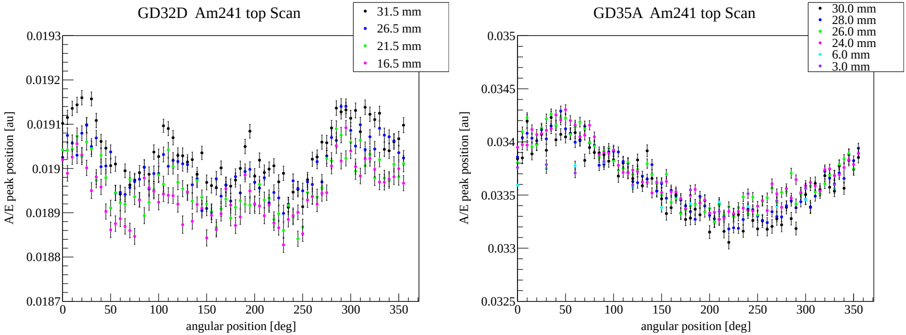

More about the detailed ^{241}Am Measurements

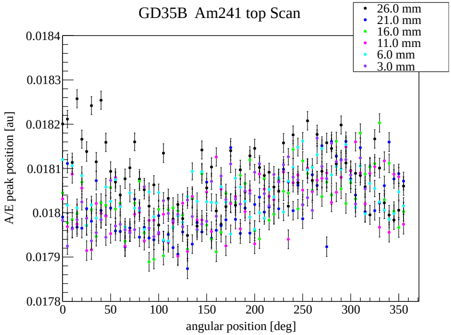

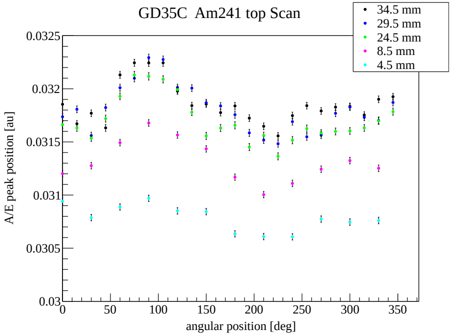

More about HV ^{241}Am Scans

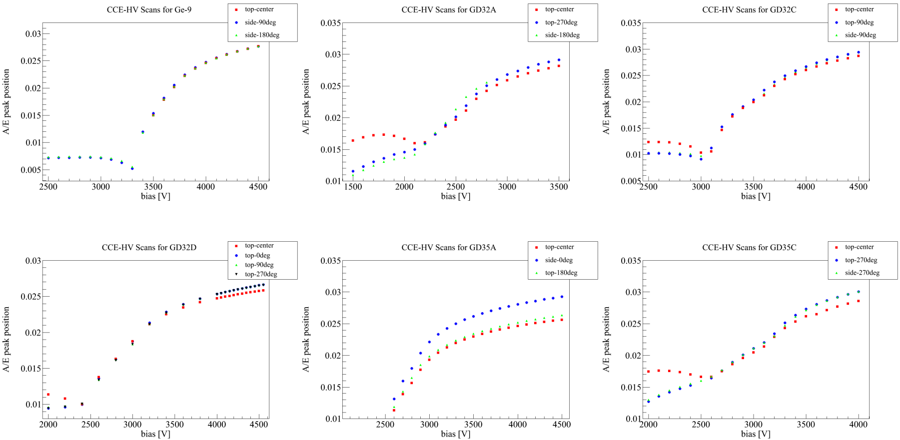

No hint that BEGe detectors are not fully depleted.

More about the comparison of PSD with and without PL I

PSD efficiencies for GD32A

	GDL	HADES
DEP	0.900 ± 0.024	0.900 ± 0.013
FEP 1.6MeV	0.150 ± 0.032	0.180 ± 0.009
SEP	0.082 ± 0.015	0.121 ± 0.006
FEP 2.6MeV	0.115 ± 0.011	0.163 ± 0.001
2004-2074 keV	0.380 ± 0.031	0.427 ± 0.004)
1989-2089 keV	0.380 ± 0.030	0.427 ± 0.003

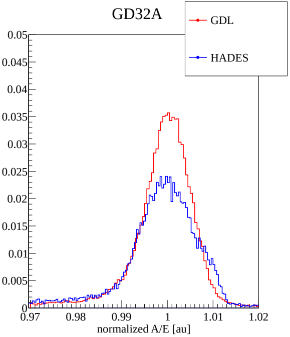

Observation:

- improvement of PSD efficiency by removing PL

More about the comparison of PSD with and without PL II

PSD efficiencies for GD35A

	GDL	HADES
DEP	0.900 ± 0.048	0.900 ± 0.023
FEP 1.6MeV	0.195 ± 0.032 ± 0.177	0.128 ± 0.013
SEP	0.085 ± 0.014 ± 0.194	0.078 ± 0.013
FEP 2.6MeV	0.116 ± 0.002 ± 0.266	0.132 ± 0.012
2004-2074 keV	0.415 ± 0.008 ± 0.202	0.400 ± 0.021)
1989-2089 keV	0.410 ± 0.006 ± 0.206	0.395 ± 0.020

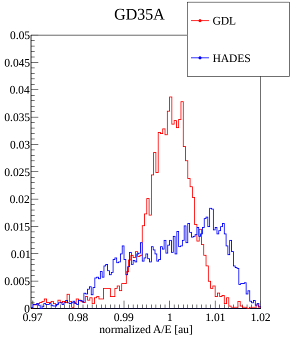

Observation:

- very low statistics
- uncertainties over estimated
- improvement in A/E distribution

More about the operation of BEGe detectors in LAr

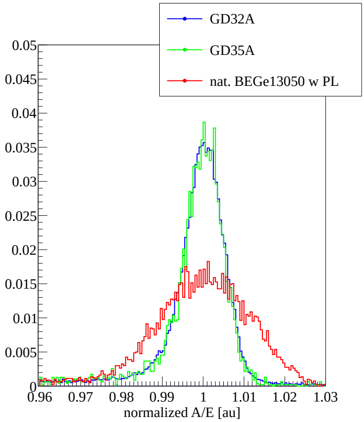

Observations:

Improvement of A/E resolution is not connected to the measurement setup!

More about the comparison between PSA performance in vacuum cryostat and the GERDA LAr cryostat

Detector	A/E resolution LAr	A/E resolution vacuum	FWHM at 2.6MeV [keV] LAr	FWHM at 2.6MeV [keV] vacuum
GD32B	1.5 %	0.8 %	2.94 ± 0.02	2.04 ± 0.02
GD32C	1.7 %	1.3 %	2.85 ± 0.02	2.46 ± 0.01
GD32D	1.6 %	1.6 %	3.00 ± 0.03	2.41 ± 0.02
GD35B	1.9 %	0.6 %	3.99 ± 0.04	2.45 ± 0.02
GD35C	1.7 %	1.7 %	3.22 ± 0.04	2.41 ± 0.02

Observations:

- energy resolution worse in GERDA than in HADES
- all A/E distributions are broadened
- resulting in worse pulse shape discrimination efficiencies

More about the A/E distributions measured in GERDA

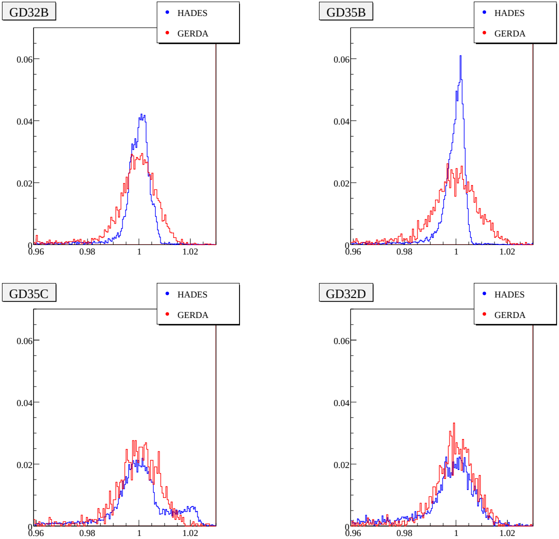

Observations:

In GERDA the level of noise is higher. A/E resolutions of all five BEGe detectors are compatible and no structure in A/E is seen.

More about the PSD efficiencies obtained in GERDA LAr cryostat

Pulse Shape Discrimination Efficiencies (calibration 1 + 2)	GD32B	GD32C	GD32D
DEP	0.900 $\pm$ 0.035	0.900 $\pm$ 0.033	0.901 $\pm$ 0.052
FEP MeV	0.187 $\pm$ 0.024 $\pm$ 0.045	0.146 $\pm$ 0.024 $\pm$ 0.027	0.163 $\pm$ 0.043 $\pm$ 0.031
SEP	0.110 $\pm$ 0.012 $\pm$0.031	0.106 $\pm$ 0.011 $\pm$ 0.027	0.108 $\pm$ 0.019 $\pm$ 0.045
FEP 1.6 MeV	0.136 $\pm$ 0.002 $\pm$ 0.055	0.131 $\pm$ 0.002 $\pm$ 0.030	0.136 $\pm$ 0.003 $\pm$ 0.061
2004-2074 keV	0.434 $\pm$ 0.008 $\pm$ 0.061	0.440 $\pm$ 0.008 $\pm$ 0.040	0.448 $\pm$ 0.011 $\pm$ 0.072
1989-2089 keV	0.435 $\pm$ 0.007 $\pm$ 0.060	0.441 $\pm$ 0.006 $\pm$ 0.040	0.449 $\pm$ 0.009 $\pm$ 0.073

Pulse Shape Discrimination Efficiencies (calibration 1 + 2)	GD35B	GD35C
DEP	0.900 $\pm$ 0.055	0.900 $\pm$ 0.059
FEP 1.6 MeV	0.168 $\pm$ 0.040 $\pm$ 0.217	0.147 $\pm$ 0.066 $\pm$ 0.114
SEP	0 0.120 $\pm$ 0.020 $\pm$ 0.214	0.128 $\pm$ 0.026 $\pm$ 0.125
FEP 2.6 MeV	0.164 $\pm$ 0.003 $\pm$ 0.269	0.172 $\pm$ 0.005 $\pm$ 0.168
2004-2074 keV	0.472 $\pm$ 0.011 $\pm$ 0.192	0.475 $\pm$ 0.015 $\pm$ 0.139
1989-2089 keV	0.472 $\pm$ 0.009 $\pm$ 0.191	0.479 $\pm$ 0.012 $\pm$ 0.140

uncertainties overestimated

Observation:

- Huge uncertainties
- Discrimination efficiency for Agamennone worse than in HADES